#### CONFERENCE PRE-PRINT

# TESTING TUNGSTEN PLASMA FACING COMPONENTS IN WEST AND AUG TOKAMAKS: LESSONS FOR ITER

Y. CORRE CEA, IRFM Saint-Paul-lez-Durance, France Email: yann.corre@cea.fr

M-H AUMEUNIER, J. BUCALOSSI, M. DIEZ, A. DURIF, A. EKEDAHL, N. FEDORCZAK, M. FIRDAOUSS, E. GAUTHIER, J. GERARDIN, J. GUNN, E. JOFFRIN, A. HUART, J. HILLAIRET, P. MAGET, M. MISSIRLIAN, C. REUX, M. RICHOU, Q. TICHIT, E. TSITRONE CEA, IRFM

Saint-Paul-lez-Durance, France

#### J. GASPAR, Y. ANQUETIN

Aix Marseille University, CNRS, IUSTI, Marseille, France

#### K. KRIEGER

Max-Planck-Institut für Plasmaphysik, 85748 Garching b. München, Germany

# S. RATYNSKAIA, K. PASCHALIDIS, T. RIZZI, P. TOLIAS

Space and Plasma Physics - KTH Royal Institute of Technology, SE-10044, Stockholm, Sweden

# R. DEJARNAC, A. PODOLNIK

Institute of Plasma Physics, Czech Academy of Sciences, 182 00 Prague, Czech Republic

# A. HAKOLA

VTT Technical Research Centre of Finland Ltd., PO Box 1000, 02044 VTT, Finland

#### C. MARTIN

Aix Marseille Univ, PIIM UMR 7345, F-13397 Marseille, France

#### R. A. PITTS

ITER Organization, Route de Vinon-sur-Verdon, CS 90 046, 13067 Saint-Paul-Lez-Durance Cedex, France

#### M. WIRTZ

Forschungszentrum Juelich GmbH, Institute of Fusion Energy and Nuclear Waste Management – Plasma Physics (IFN-1), 52425 Juelich, Germany

# B. ESPOSITO, M. REGINE, C. MONTI

Dipartimento Nucleare, ENEA, C.R. Frascati, Via E. Fermi 45, Frascati, I-00044 Roma, Italy

# Abstract

Next step fusion devices will face unprecedented heat loads and particle fluence with thousands of hours of plasma exposure on plasma-facing components (PFC) and gigajoules of energy to extract in a single discharge. These components must guarantee acceptable lifetime, reliable heat exhaust capabilities (10-15 MW/m² power fluxes in steady state) and a high level of resilience after multiple thermal stresses generated by combined steady-state heat loads and transient events, such as ELMs or disruptions. An extensive tungsten (W) PFC testing work-program has been conducted in the WEST (Tungsten Environment in Steady State Tokamak) and ASDEX Upgrade (AUG) tokamaks, taking advantage of key capabilities and strengths of the two machines. WEST is a superconducting tokamak with long pulse duration capabilities currently equipped with an ITER-grade actively cooled divertor, including shaped monoblocks (MB) with the 0.5 mm height toroidal bevel as foreseen for ITER, while AUG allows the exposure of dedicated tile-sized samples (with different geometries, gap size, slopes and materials) in ELMy H-mode discharges using its divertor manipulator DIM-II system. The first part of the paper reports on the operation of the ITER-grade PFC in WEST since the commissioning of the divertor in 2022. The second part of the paper presents dedicated experiments performed in AUG and WEST in order to study W failure modes, W melting across toroidal gaps (during sustained or transient melting) and impact of the runaway electrons on W material. The results reported here provide new information on W material response (e.g. heating, cracking or melting) of direct relevance to ITER.

# 1. INTRODUCTION

With the new ITER baseline, Tungsten has been selected to cover the divertor region and also the main chamber. Despite the high melting point of tungsten (~3400°C), failure and melting accident could happen during plasma operation because of the very high level of power foreseen in the plasma and also because of the large number of systems, sub-systems that are required to operate safely the tokamak. Efficient and reliable Plasma Facing Component (PFC) operation is therefore required to ensure full and optimum use of the tokamak device. One of the research topics of the EUROFUSION program is currently the investigation of the operational limits and lifetime affecting processes for the PFCs at first wall areas exposed to high heat and particle fluxes, with a focus on metallic devices. The scientific objectives are to quantify power distributions on castellated and shaped PFCs and to assess the impact of transient heat loads, such as Edge Localized Modes (ELMs) or disruptions, and sustained high power / high particle fluence plasma exposure on the thermo-mechanical properties of metallic PFCs. A particular focus is also given to open issues associated with the new ITER baseline, such as the impact of the Runaway Electrons (RE) on tungsten material and tungsten melting across toroidal gaps on castellated components. The paper shows the recent experiments performed in WEST and AUG tokamaks to address these issues. Section 2 presents the operation with the ITER grade PFCs during WEST experimental campaigns (from C6 experimental campaign in 2022 up to C11 experimental campaign achieved in 2025). Section 3 shows the cracking of the tungsten observed in the high heat load areas in the WEST ITER grade divertor and the plasma exposure of one pre-damaged block with a deep crack propagating from the loaded surface in the direction of the cooling pipe (generated in a HHF test facility with repeated steady high heat load). Section 4 presents two experiments designed to investigate tungsten melting across toroidal gaps, one was performed in AUG with the divertor manipulator (transient melting) and the other one was performed on the ITER grade divertor in WEST (sustained melting). The last section (5) presents the RE impact experiment performed on the W-tiles of the inner bumper in the WEST tokamak.

# 2. ASSESSING HEAT LOADS ON CASTELLATED AND SHAPED COMPONENTS

### 2.1. WEST operation with the fully actively cooled ITER divertor

The WEST program is focussed on assessing the performance of the ITER actively cooled tungsten (W) divertor under tokamak operation in full metallic environment [1]. The second phase of the WEST project started in December 2022 with the lower divertor entirely made of actively cooled ITER-grade tungsten mono-blocks. ITER-grade refers to the W materials which comply with the ITER divertor requirements in terms of chemical composition, density, hardness as well as grain size and elongation. The ITER technology for the divertor consists of bulk tungsten (W) monoblocks (MBs) bonded on a CuCrZr cooling tube, with  $\approx 0.5$  mm toroidal gaps between blocks [2]. The heat exhaust capability provided by the pressurized water-cooling circuit are  $10 \cdot MW.m^{-2}$  steady state, up to  $20 \cdot MW.m^{-2}$  for slow transients (for a limited number of cycles). The PFCs for the WEST divertor were manufactured by AT&M (Advanced Technology of Materials, China) company using hot isostatic pressing (HIP) for bonding W blocks (armour thickness 6 mm) to CuCrZr tube with a Cu-OFHC interlayer.

The WEST lower divertor consists of 456 PFCs, each of them having 35 W blocks for which the width varies between 26 and 31 mm in the toroidal direction, from the inner to the outer parts of the PFC, respectively. In total, the divertor target includes 15.960 W blocks, which represents about 5% of the number of MB foreseen in the ITER divertor. The MBs are shaped on the inboard and outboard part of the divertor (not on the private flux

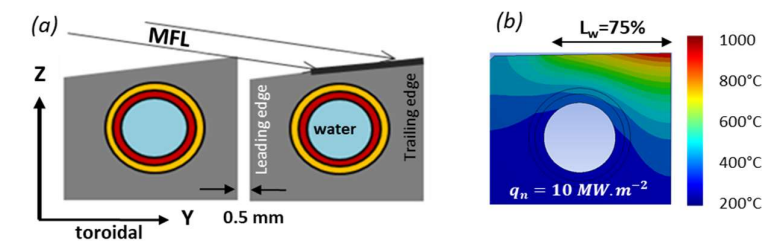


FIG. 1. (a) cross-section of the MB with the 0.5 height toroidal bevel showing the wetting area (broad line). (b) Temperature distribution computed with nominal heat loading condition (wetted area = 75%, 10 MW.m<sup>-2</sup> uniformly distributed in the poloidal direction)

area) with the 0.5 mm height toroidal bevel to protect the poloidal LE from excessive heat load due to the almost perpendicular incidence of the magnetic field lines (MFLs) on the LE surface [3]. The main drawback of the toroidal bevel is the reduction of the wetted area and the increase of the MFLs surface inclination angle compared to flat top geometry ( $\alpha = \alpha_0 + 1^\circ$ , where  $\alpha_0$  is the incidence angle with flat top geometry) [4], see figure 1 (a). The

geometry is defined in the local frame of the PFU  $\{x, y, z\}$ , where x, y and z correspond to the poloidal, toroidal and vertical directions, respectively. The geometrical projection of the parallel heat flux onto MB surfaces predicts  $\approx 20\%$  higher heat flux on the top surface with the bevel geometry compared to the flat top geometry [5]. Furthermore, vertical misalignment between PFU may change the wetted area and consequently, the surface temperature distribution in the toroidal direction [6]. The nominal situation in ITER, assuming  $\alpha$ =3.5° and perfect alignment of the PFCs ( $\delta_v$ =0), corresponds to 75% wetting of the top surface, see figure 1 (b). The tolerances for PFC assembling have been set by ITER to  $\pm 0.3$  mm vertical misalignment between two consecutive PFCs ( $\delta_v$ ) to

prevent overexposed LE. Assuming incident angle of  $\alpha=3.5^{\circ}$  as measured in WEST, the maximum and minimum wetted areas would be 90% and 60% respectively. The temperature distributions in the toroidal direction are reported in [6] for different wetted areas. In the nominal case (75% of the surface wetted under 10 MW.m<sup>-</sup> <sup>2</sup> plasma load), the surface temperature computed at the trailing and leading edges are 1000°C and 300°C respectively, leading to 700°C temperature gradient in the toroidal direction. A Very High spatial Resolution (VHR) Infra-Red (IR) system (0.1mm/pixel) has been installed to study the heat load at the MB scale of [7]. Figure 2 (a) shows the temperature distribution on two consecutive blocks, at the OSP position, as measured by the VHR IR system during WEST plasma operation. Figure 2 (b) shows the toroidal temperature profile, with the hot and cold parts of the block, in the wetted and magnetically shadowed areas, respectively. In WEST, the assembling of the PFCs is controlled by surface metrology before and after welding of the cooling pipes. In-situ laser scanning surface metrology1 has been performed on the lower and upper divertor rings

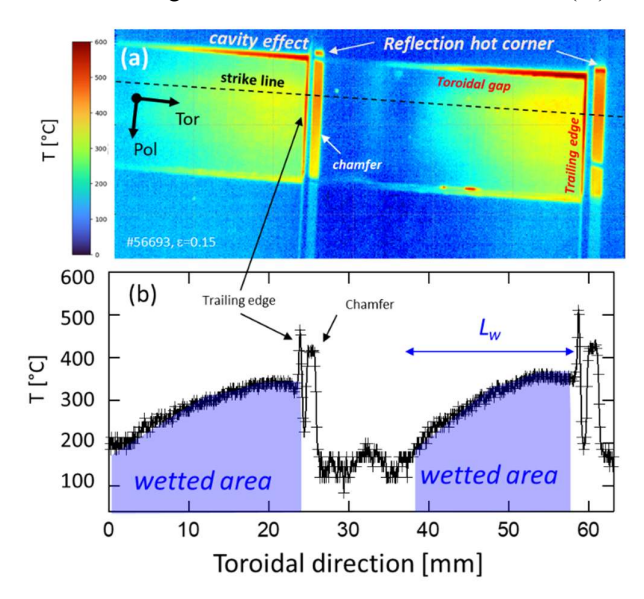


FIG. 2: (a) Temperature distribution measured with the VHR IR System (nominal wetted area = 75%). (b) toroidal temperature profile taken along the separatrix

after the completion of the WEST phase 2 project. The surface metrology shows maximum discrepancy up to 1 mm between the measurement and the theoretical 3D Computer Aid Design (CAD) model. The vertical steps between two consecutive components are computed afterward. At the end of the assembling, 100% of the blocks complied with the assembly  $\pm 0.3$  mm tolerances in the high heat flux areas for the standard divertor sectors. Higher misalignments have been introduced on purpose on the test divertor sector (up to 0.5 mm positive and negative vertical misalignments). The inclination of the top surface of the blocks have also been controlled. The analysis reveals deviation up to 1° compared to the theoretical value (1° due to the 0.5 mm bevel). These misalignments are then included in the CAD model of the PFCs in order to simulate the heat load distribution on the divertor sector. Surface tilting leads to ± 20% variation of the heat load compared to the nominal case (no tilting) combined with a variation of the wetted fraction (in particular when the incident angle is small, as expected in the minimum heat flux areas due to the toroidal magnetic field modulation). Accurate surface metrology is therefore mandatory during the PFC assembling in ITER, in particular in the inner and outer strike point areas where high heat loads are expected. The surface temperature also varies in the poloidal direction due to the heat flux distribution in the Scrape-Off Layer (SOL). The heat flux is very sharp on the Private Flux Region (PFR) side and follows exponential decay in the SOL side due to turbulence and neoclassical perpendicular transport of particles. The heat flux distribution in the poloidal direction could be modelled with a convolution of an exponential with a Gaussian characterized by two physical parameters: the spreading factor in the PFR (s) and the heat flux decay length ( $\lambda_q$ ). Recent studies performed in WEST show the presence of two characteristic lengths in the outer part of the SOL, in particular during high power operation [8]. The first part of the SOL power could be characterized by a narrow component (λ<sub>q</sub> between 2 and 10 mm reported on the target), while the second part of the SOL power could be characterized by broader one ( $\lambda_q$  between 10 to 50 mm also reported on the target). The decay of the power in the poloidal direction leads to a decay of the surface temperature in the same direction, in particular on the most loaded blocks near the separatrix because of the narrow component which is lower than the block width of 12 mm. During plasma operation, the surface temperature of the blocks depends of the peak heat load first, but also the strike line position on the top surface. On the Outer Strike Point (OSP), more power

<sup>&</sup>lt;sup>1</sup> Hexagon Absolute Arm 8525-7-6976-FA (laser scanner Hexagon RS6-0407-GE with 0.047 mm accuracy).

will be delivered to the block if the strike line is on the inner side of the block, while the same power will split over two blocks if the strike is located on the outer part of the block. The temperature distribution on the MB scale has been computed in the nominal case for WEST (75% wetted area, heat load of 10 MW.m<sup>-2</sup>, strike line on the outer part of the block and heat flux decay length of 5 mm, narrow channel). The modelling reveals temperature gradients in the poloidal (~200°C) and toroidal (~700°C) direction respectively, which is clearly unfavourable for thermo-mechanical handling of the component. Because of the magnetic field and the bevel geometry, the tokamak loading conditions are very different from standard High Heat Flux (HHF) testing conditions where the beam power is uniformly distributed on the wetted area (it is for instance not possible to reproduce the heat flux decay length). Both tokamak and HHF devices are complementary to achieve complete PFC testing program for next step fusion device. Assessing the thermal loads and potential material damages (tungsten recrystallization, cracking and melting) on ITER-grade components is a key point for safe operation and divertor lifetime. Three experimental campaigns have been achieved in WEST phase 2 with the fully actively cooled ITER grade divertor. Table 1 summarizes the WEST phase 2 operation covering this period. About 4000 plasmas were performed which represents about 18 hours of total plasma cumulated time. More than 2400 disruptions have been counted. The WEST plasmas are mainly characterized by steady state plasma conditions in the L-mode regime with attached divertor plasma conditions, where the electron temperature (Te) lies between 20 and 40 eV on both inner and outer legs of the divertor. In the last experimental campaign, highly radiative plasmas, X-Point Radiator (XPR) scenario based on nitrogen seeding, were also performed with low temperature at the divertor target (T<sub>e</sub> < 10 eV). Low temperature plasmas at the edge are still marginal compared to attached plasma condition (XPR pulses represents 10% of the total pulse number in C10-C11). Post-mortem measurements reveal  $25 \pm 5 \,\mu m$  net erosion on the outer strike point and 300 µm thick deposits on the inner part of the divertor (few MB away from the ISP), which is consistent with intensive erosion of the targets in attached plasma condition

	Nb Plasma	Cum. time (h)	Disruptions	W total (GJ)
C6-C7 July 2022-April 2023	1160	5.5	702	43.5
C8-C9 Dec. 2023 – April 2024	1299	5.7	817	38.9
C10-C11 Jan – April 2025	1583	7	945	41.8

Table 1: Overview of the WEST experimental campaigns: number of plasma discharges, cumulated plasma duration, disruption and injected energy during WEST phase II.

In WEST, the maximum RF power injected and coupled to the plasma, in a stable and reliable way (RF heating duration higher than 5s), is 5.5 MW, mainly with Lower Hybrid launchers (LHCD heating system). Higher power has been coupled to the plasma during shorter duration because of plasma instabilities, leading to MHD activity, arcing and radiative collapse. Accurate measurement of the tungsten temperature is required in order to evaluate the heat load on the PFUs. WEST is equipped with an extensive set of diagnostics for heat load measurements. Infrared thermography systems have been deployed on the top part of the machine to monitor the temperature of the component on the lower divertor. They currently consist of five endoscopes providing a broad view of the divertor sectors with a spatial resolution ranging between 3 and 5 mm per pixel and one endoscope with a reduced field of view (few MBs) at a Very High spatial Resolution (VHR) of 0.1mm/pixel [7]. Because of the low emissivity of tungsten, which depends on various parameters such as temperature, surface structure and chemical composition, it is very challenging to derive the PFU temperature during plasma experiments [9]. To complete the IR thermography, some PFUs are equipped with embedded temperature sensors such as thermocouples (TCs) and multiplexed fiber Bragg gratings (FBGs), which provide up to 11 and 15 spot measurement points per fiber 5 mm below the surface on the trailing edge [10]. The TC and FBG measurements are therefore unsensible to surface effects such as emissivity of the tungsten or presence of deposited layer. The drawback of the TC and FBG systems is the time response of the measurement which is longer (in the range of 5s to 20s) than the time needed to reach the thermal equilibrium of the block (5s). They provide accurate temperature measurements for plasma discharges

with 10s steady-state at least. The experimental heat load data base obtained in WEST with the FBG measurements on the OSP is in the range of interest for ITER divertor testing (5 – 12 MW.m<sup>-2</sup>), see Figure 3 (a). The heat load measured on the inner strike line is broader and the peak value is typically a third of the value obtained on the OSP (few MW.m<sup>-2</sup>). The recent progress made in term of steady-state tokamak operation [11] (plasma

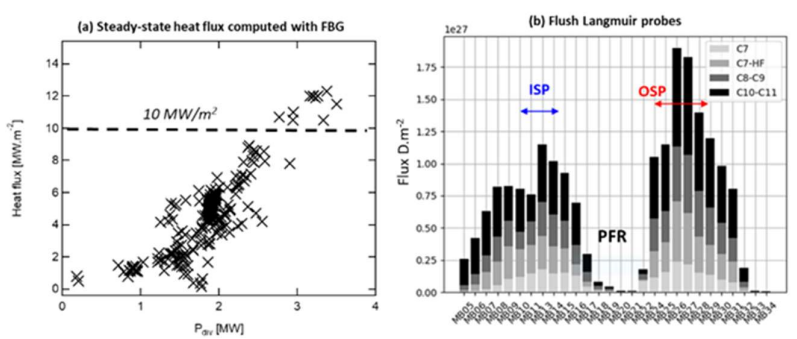


FIG. 3. (a) heat load calculated on the ITER-grade PFU with multiplexed FBG sensing diagnostic as function of the power in the SOL. (b) distribution of the deuterium fluence over the monobloc position in the device (poloidal direction)

duration and injected RF energy) enables to reach high particle fluence on the divertor target. The D<sup>+</sup>-fluence is computed with the Flush-mounted Langmuir probes radially distributed in the maximum heat flux areas on the inner and outer parts of the divertor. The D<sup>+</sup> flux measured on each block has been integrated pulse by pulse during the three experimental campaigns. The total accumulated fluence during the C6-C11 campaigns are in the range of  $0.9-1.2 \times 10^{27}$  D<sup>+</sup>.m<sup>-2</sup> and  $1-1.75 \times 10^{27}$  D<sup>+</sup>.m<sup>-2</sup> in the inner and outer divertor legs respectively, which corresponds to several ITER pre-fusion operation pulses ( $2 \times 10^{26}$  D<sup>+</sup> m<sup>-2</sup> per pulse) [12], see figure 3 (b).

#### 2.2. Heat load in gaps and leading edges: prediction and observation

The 0.5 mm toroidal bevel offers good protection of the poloidal LE, this is now demonstrated in the WEST tokamak. Post-exposure observations performed in WEST, during the two previous shutdowns, show no more W-cracking on the LE has previously observed with the flat top geometry [13]. However, magnetic field lines can penetrate in the toroidal gaps and strike the LE with a ~90° incidence on sharp LE geometry (as foreseen in ITER) and ~45° on chamfered geometry (as used in WEST), such particular feature is also called "Optical Hot Spot" (OHS) [6]. Numerical predictions indicate possible high heat fluxes in ITER, on the OHS first but also in the toroidal gap because of the Larmor gyration of the ions around the magnetic field lines, especially during transient events such ELMs, which can lead to material damages [5]. The local distribution of the ion flux on the toroidal gap side was quantified in AUG by pre- and post-exposure analysis of platinum marker layers installed in a dedicated castellated target components with the DIM-II divertor manipulator [14]. The depth extent of the erosion patterns agrees with expected values and parametric dependencies from Larmor orbit size during Type-I ELM scenario.

To better visualize and study the OHS in WEST, a  $\delta_p$ =1.5 mm poloidal misalignment was introduced between two consecutive PFUs, see figure 4. For 10 MW.m<sup>-2</sup> surface heat loading condition as reported in WEST, the heat loads on the sharp LE and 45° chamfer are expected to be 200 MW.m<sup>-2</sup> (ITER case) and 145 MW.m<sup>-2</sup> (WEST case). In WEST, the temperature prediction for the OHS is 460°C with the chamfer, while similar prediction with sharp LE leads to 600°C during steady state plasma operation at nominal power on very small surface. A toroidal gap (TG) experiment has been

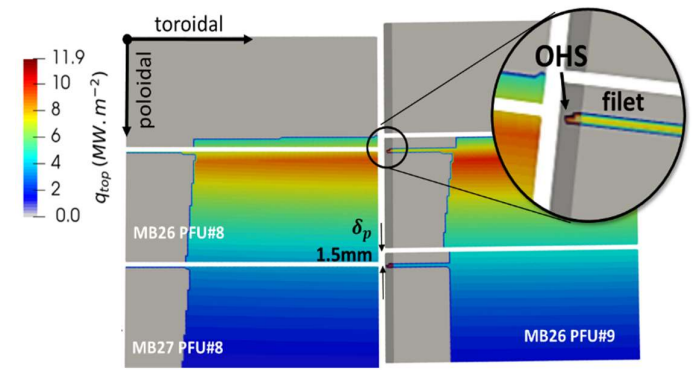


FIG. 4. Heat load simulation with the field line tracing code PFCflux with 1.5mm poloidal misalignments between two consecutive ITER-grade PFU.

performed to investigate the heat load distribution in the TG of the W-block with the VHR IR system. L-mode discharges (Ip = 400 kA) with high power (4.5 MW LH) were performed with the outer strike line aligned with the TGs. High apparent temperatures were measured in the TGs compared to the MBs top surface, see figure 2 (a). The high temperature observed in the TGs are attributed to the multiple reflections occurring between metallic surfaces facing each other (phenomenon called the "cavity effect"). An extensive set of numerical codes have been developed and used to reproduce the complex thermal scene with the 3D monoblock: MLFs tracing code to predict heat loads on PFCs, Finite Element Methods to calculate the resulting surface temperature, camera model to account for the pixel size and field of view, Monte Carlo ray tracer to simulate infrared images by taking into account the low emissivity of tungsten and multiple reflections [15]. The cavity effect observed with the VHR IR camera is very well reproduced in the TGs. Specular reflection is found to play a major role on the trailing edges and poloidal chamfer which are located in the magnetically shadowed areas (very close to the "hot" upstream block), see figure 2 (b). Due to the reflections on the poloidal chamfer, it was concluded that the OHS is not measurable. The hot spot pattern observed experimentally in the cold areas is reproduced with the emission and reflection modelling of the W surfaces. In summary, temperatures are overestimated in the cold areas because of specular reflection, and underestimated on the hot surfaces because of the low surface emissivity. This should be considered during the monitoring of the surface temperature with the IR system in ITER.

#### 3. TUNGSTEN CRACKING

Modification of the divertor sectors (PFU replacement) and PFC inspection take place during every shutdown. One of the most important damages observed during WEST phase 1 operation, running with the first series of ITER grade PFCs with the flat top geometry, was systematic cracking of the LE where the maximum heat flux areas is applied [16]. The WEST phase 2 operation has demonstrated that the toroidal bevel offers a good protection of the poloidal LE, no more LE cracking is reported.

However, spontaneous cracking was observed on the wetted areas of the top surface. The cracks appeared rapidly, after the first (C6-C7) experimental campaign. Cracking was also observed during the following shutdowns after the second (C8-C9) and third (C10-C11) experimental campaigns, even on new PFCs introduced on the WEST divertor. The crack-networks are

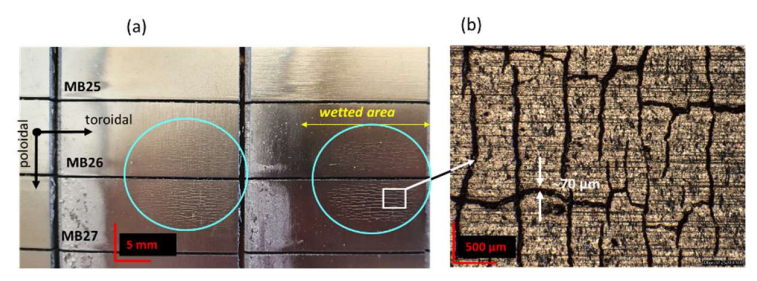


FIG. 5. Post-C9 visual inspection (a) and optical microscopy (b) in the crack area (shown in cyan).

observed in the high heat load areas, near the outer strike point and preferentially placed on the most loaded components, see figure 5 (a). The crack width measured with optical microscopy is in the range of 40 to 90 µm, figure 5 (b). Tungsten cracking is not expected with the steady state heat load measured in WEST, transients such as disruptions events could be involved, as for the LE cracking previously observed with the flat top geometry [17]. To understand the failure mechanism, a new component, non-exposed in WEST, has been tested in the HADES HHF facility to reproduce the thermal shock of the disruption. Three hundred thermal cycles have been performed with medium sized disruption (80 MW.m<sup>-2</sup> applied during 3.3ms, 6.6ms, and 9.9 ms to test different impact factors) on cold and pre-heated blocks to mimic the impact of disruption-like impact away from the strike line and near the strike line respectively. About 75% of the block surface was exposed to the beam to mimic the toroidal bevel effect in the tokamak. No cracking was observed. The electron beam power has also been used up to 140 kW to achieve high heat load, up to 160 MW.m<sup>-2</sup>. The thermal response of the MB measured with fast IR camera shows temperature increase up to 700°C and still, no crack was observed.

To test the ageing of the ITER-grade components on an accelerated basis, three PFCs have also been taken out from the production batch and exposed in a HHF test facility (e-beam gun) to generate well controlled and different type of damages. Three generations of predamaged components have been developed and exposed to WEST plasmas (through C3 to C11 experimental campaigns). The third generation of pre-damaged PFC includes a deep crack generated by repeated steady-state high heat load (24 MW.m<sup>-2</sup>). It was installed in WEST during the shutdown S7 (2023) and exposed to the WEST plasma during the C8-C11 experimental campaigns (2024-2025). It features a deep crack extending in the direction of the cooling pipe, crack width in the range of 60 - 120 μm, with full poloidal extension over the block.

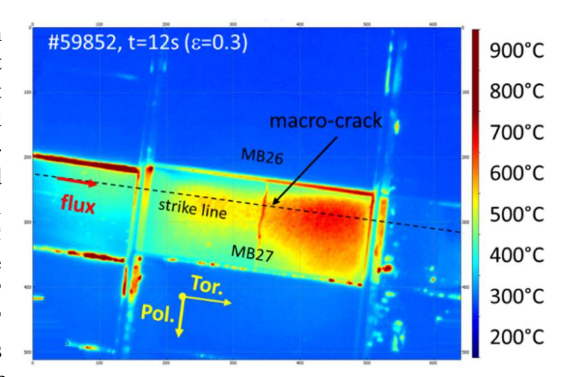


FIG 6. VHR IR image of the macro-crack during WEST operation

The crack exhibits a narrow leading edge (LE) exposed to the incident parallel heat flux. A dedicated experiment was conducted to reach maximum heat loading conditions on the macro-crack using the VHR IR system. The crack is clearly visible in the center of the VHR IR image thanks to the cavity effect (multiple reflections inside the crack leading to enhanced emissivity), see figure 6. No evolution of the crack width or abnormal thermal behavior were observed. The heat exhaust capabilities remain unchanged (rising and cooling time are similar to healthy component) and no deleterious evolution of the crack LE was observed.

## 4. TUNGSTEN MELTING ACROSS TOROIDAL GAPS

Melting experiments were carried out in AUG and WEST tokamaks to investigate the melt displacement in the toroidal gaps (0.5 mm) between blocks and benchmark melt code simulations. Penetration of the melt into the gaps could have important consequences on the PFU mechanical response, especially under strong electromagnetic loads in the course of major disruptions [18]. Transient melting of specially designed tungsten samples featuring toroidal gaps has been achieved in ASDEX Upgrade providing direct evidence of gap bridging, Fig. 7 (a). The post-mortem analysis of exposed samples reveals apparent poor wetting and the weak attachment of re-solidified melt. This is a consequence of prompt re-solidification on the cold surface across the gap which limits melt spreading. Sustained melting has also been achieved in WEST on a poloidal LE of the actively cooled ITER-grade block, Fig. 7 (b). Eight seconds of sustained melting were achieved in one discharge. A resolidified melt droplet observed in the gap is of the mm size and can reach the adjacent blocks. Both post-mortem observation and melt dynamic simulation show that gap bridging is the main mechanism for melt transport through

the toroidal gap. The MEMENTO code was able to reproduce the thermal responses and melt deformation profiles, due to JxB forces (where J is the replacement current generated by the thermoionic emission), for the two experimental cases: 20 cm.s<sup>-1</sup> melt velocities and pool depth of several tens of µm during transient melting in AUG compared to viscous and slower melt displacement of few cm.s<sup>-1</sup> with ultra-thin ~ µm layers during sustained melting in WEST. The empirical evidence from transient and sustained melting and simulations reveal that the

# (a) Transient melting in AUG intra ELM 900 MW.m² 3.0e+22 1000 1500 200 2.6e+33

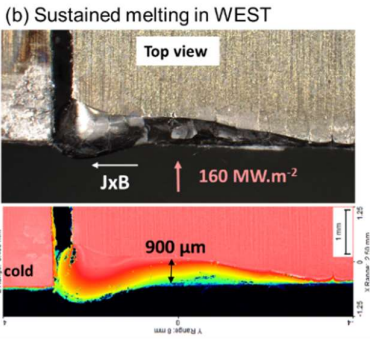


FIG 7: (a) Transient melting in AUG post-mortem (top) and modelling (bottom, H-mode) reproduced with permission from [18]. (b) Sustained melting in WEST on actively cooled ITER grade block post-mortem.

presence of gaps can be ignored in macroscopic melt motion predictions as well as that the re-solidification limited melt spreading facilitates gap bridging without wetting of the inner gap. This also leads to poor melt attachment.

#### 5. TUNGSTEN DAMAGES INDUCED BY RUNAWAY INCIDENCE

The impact of the Runway Electrons (RE) with material components lead to deep energy deposition, even inside dense material with high atomic number such as W, and severe damages as observed in many tokamaks (material fragmentation, melting and projection). RE usually starts during early phase of the plasma start-up (current and density ramp-up) and immediately after disruptions. Significant progress in RE generation, control and mitigation have been performed in WEST during phase 2 operation phase. Empirical data from controlled experiments are necessary to understand the underlying physics and validate modelling efforts. A first controlled RE impact experiment has been performed on WEST with dedicated instruments to infer the RE energy and pitch angle (Runaway Electron Imaging Spectroscopy [19]), the RE impact duration with the inner bumper and emission of debris (tangential view fast visible camera 2 kHz) and power loading to the bumper during the impact (embedded thermocouples, tangential view fast IR camera 4 kHz). Two consecutive impacts have been achieved with 230 kA RE current toward the instrumented tile (located 20 cm above the midplane), Important damage is observed immediately after the impact, see figure 8 (a) and (b) and during the visual inspection, figure 8 (c). The impact duration is estimated with fast cameras (2.5ms). The RE energy (17 MeV) and pitch angle (in the range of 0.15-

0.3 radians) are estimated under the assumption of monoenergetic RE distribution, with the synthetic synchrotron radiation diagnostic tool SOFT [20] by comparison with experimental data. These experimental data will be used as input to validate the work-flow (GEANT4 - MEMENTO/LS-DYNA) to test predictive capabilities for ITER.

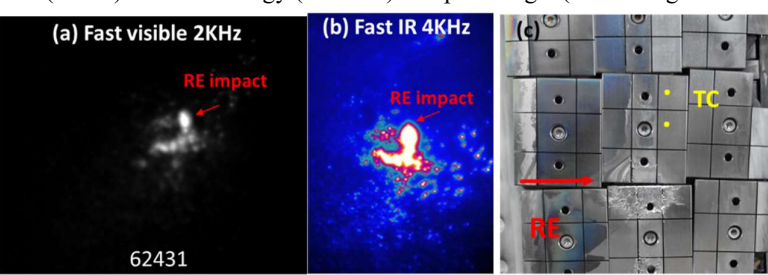


FIG 8: RE impact view by fast visible (a) and fact IR camera (b) at the end of the RE. (c) picture of the inner bumper with the impact of the RE.

# 6. CONCLUSION

A large number of ITER-grade tungsten blocks (15960 to cover the lower divertor ring) have been tested in WEST during significant plasma exposure (18 hours in total). The blocks located in the high heat flux areas have been exposed to ITER relevant heat flux, with peak heat flux up to 12 MW.m<sup>-2</sup> as reported on the OSP, and also ITER relevant cumulated deuterium fluence (equivalent to few ITER PFPO pulse). No major failure and no evolution of the heat exhaust capabilities have been observed in the ITER grade divertor tested in WEST. The effect of the toroidal bevel geometry has been assessed in WEST with the very high spatial resolution (VHR) IR camera (0.1 mm/pixel). At the Monoblock scale, IR data interpretation requires dedicated photonic modelling because of multifaceted and highly reflective thermal scene. Specular reflection is found to be dominant in toroidal gaps, trailing edges and chamfered surface. Unexpected cracking is observed on top surface in the high heat flux area only, near the outer strike point. Simulated disruptions performed in HHF test don't reproduce the experimental observations in the tokamak. Combined thermomechanical effects due to "transient", potential residual stresses in the micro-scale surface due to surface machining of the bevel and plasma induced-effect are suspected. Further numerical and experimental studies are required to understand the damage mechanism. Exposure of deep macro-

crack pre-damaged block in WEST show no significant degradation/evolution of the damage during plasma operation. Controlled tungsten melt transport across PFC gaps have been performed in AUG and WEST in different plasma loading condition. The melt flow froze very rapidly after crossing the gap, which prevents the melt from revolving into the gap, as observed in the two experimental cases: sustained melting (ultra-thin melt layer and slow melt motion in WEST) and transient melting (deeper pool depth and faster melt motion in AUG). First controlled RE impact on W material were performed: major damage was observed despite the high melting point of W and data are available to test the predictive capabilities for ITER.

#### **ACKNOWLEDGEMENTS**

This work has been carried out within the framework of the EUROfusion Consortium, funded by the European Union via the Euratom Research and Training Programme (Grant Agreement No 101052200 - EUROfusion). Views and opinions expressed are however those of the author(s) only and do not necessarily reflect those of the European Union or the European Commission. Neither the European Union nor the European Commission can be held responsible for them.

# REFERENCES

- [1] J. Bucalossi, «WEST full tungsten operation with an ITER grade,» Nuclear Fusion, p. 112022, 2024.
- [2] T.Hirai et al., «Design optimization of the ITER tungsten divertor vectical targets,» Fusion Engineering and Design, vol. 127, pp. 66-72, 2018.
- [3] Y. Corre, «Testing of ITER-grade plasma facing units in the WEST tokamak: Progress,» *Nuclear Materials and Energy*, vol. 37, p. 101546, 2023.
- [4] A.Grosjean et al., «Very High Resolution Infrared imagery of misaligned tungsten monoblock edge heating in the WEST tokamak,» Nuclear Materials and Energy, vol. 27, p. 100910, 2021.
- [5] J. Gunn, «A study of planar toroidal-poloidal beveling of monoblocks on the ITER,» *Nuclear Fusion*, vol. 59, p. 126043, 2019.
- [6] J. Gunn, «Surface heat loads on the ITER divertor vertical targets,» Nuclear Fusion, vol. 57, p. 046025, 2017.
- [7] M.Houry et al., «The very high spatial resolution infrared thermography on ITER-like tungsten monobloks in WEST tokamak,» Fusion Engineering and Design, vol. 146, pp. 1104-1107, 2019.
- [8] Y. Anquetin, «Identification of a double decay length heat flux deposition shape with embedded thermal measurement and neural network,» *Nuclear Material and Energy*, vol. 41, p. 101788, 2024.
- [9] J.Gaspar et al., «In situ assessment of the emissivity of tungten plasma facing components of the WEST tokamak,» Nuclear Material and Energy, vol. 25, p. 100851, 2020.
- [10] N.Chanet et al., «First temperature database achieved with Fiber Bragg Grating sensors in uncooled plasma facing components of the WEST lower divertor,» Fusion Engineering and Design, vol. 170, p. 112528, 2021.
- [11] R. Dumont, «WEST LONG-PULSE ACHIEVEMENTS IN SUPPORT OF NEXT-STEP FUSION DEVICES,» This conference.
- [12] S. Brezinsek, «Erosion, screening, and migration of tungsten in the JET divertor,» *Nuclear Fusion*, vol. 59, p. 096035, 2019.
- [13] J.P.Gunn et al., «Thermal loads in gaps between ITER divertor monoblocks: First lessons learnt from WEST,» *Nuclear Materials and Energy*, vol. 27, p. 100920, 2021.
- [14] K. Krieger, «Investigation of ELM-related Larmor ion flux into,» Nuclear Fusion, vol. 63, p. 066021, 2023.
- [15] A. Juven, «U-Net for temperature estimation from simulated infrared images in tokamaks,» Nuclear Materials and Energy, vol. 38, p. 101562, 2024.
- [16] M.Diez et al., «In situ observation of tungsten plasma-facing components after the first phase of operation of the WEST tokamak,» *Nuclear Fusion*, vol. 61, p. 106011, 2021.
- [17] A.Durif et al., «Cracks initiation and propagation of tungsten actively cooled ITER-like components during high power load experiment in WEST,» chez 19th International Conference on Plasma-Facing Materials and Components for Fusion Applications (PFMC), Bonn, 22 26 May, 2023.
- [18] S.Ratynskaia et al., «Experiments and modelling on ASDEX Upgrade and WEST in support of tool development for tokamak reactor armour melting assessments,» *Nuclear Materials and Energy*, vol. 33, p. 101303, 2022.
- [19] G. Ghillardi, «Study of runaway electron dynamics in FTU using synchrotron spectra and imaging measurements,» Plasma Phys. Control. Fusion, vol. 67, p. 055029, 2025.
- [20] M. Hoppe, «SOFT: a synthetic synchrotron diagnostic for runaway electrons,» *Nuclear Fusion*, vol. 58, p. 026032, 2018